Eur Biophys J (2003) 31: 626–632
DOI 10.1007/s00249-002-0263-x

ARTICLE

Albena Jordanova · Zdravko Lalchev · Boris Tenchov

Formation of monolayers and bilayer foam films from lamellar, inverted hexagonal and cubic lipid phases

Received: 6 June 2002 / Accepted: 3 October 2002 / Published online: 1 November 2002

Abstract This study revealed large distinctions between the lamellar and non-lamellar liquid crystalline lipid phases in their spreading at the air/water interface and propensity to form bilayer foam films. Comparative measurements were made for the lamellar L_α, the inverted hexagonal H_{II} and the bicontinuous cubic Pn3m phases of the phospholipid dipalmitoleoylphosphatidylethanolamine (DPoPE). With regard to monolayer formation, followed as the decrease of surface tension with time, the best spreading (lowest surface tension) was observed for the L_α phase, and poorest spreading (highest surface tension) was recorded for the H_{II} phase. The cubic Pn3m phase of DPoPE, induced by temperature cycling, retained an intermediate position between the L_α and H_{II} phases. According to their ability to lower surface tension and disintegrate at the air/water interface, the three phases thus order as $L_\alpha > Pn3m > H_{II}$. Clearly expressed threshold (minimum) bulk lipid concentrations, C_t, required for formation of stable foam bilayers from these phases, were determined and their values were found to correlate well with the bulk lipid phase behaviour. The C_t values for L_α and H_{II} substantially increase with the temperature. Their Arrhenius plots, $\ln C_t$ versus $1/T$, are linear and intersect at ~36–37 °C, coinciding with the onset of the bulk $L_\alpha \rightarrow H_{II}$ phase transition, as determined by differential scanning calorimetry. However, the C_t value for the Pn3m phase, equal to 30 μg/mL, was found to be constant over the whole range investigated between 20 °C and 50 °C. The horizontal C_t versus T plot for the Pn3m phase crosses the respective plot for the L_α phase at the temperature bounding from below the hysteretic loop of the $L_\alpha \leftrightarrow H_{II}$ transition (~26 °C), thus providing a certain insight about the thermodynamic stability of the Pn3m phase relative to the L_α phase. The established strong effect of the particular lipid phase on the formation of monolayers and stable black foam films should be of importance in various in vitro and in vivo systems, where lipid structures are in contact with interfaces and disintegrate there to different extents.

Keywords Foam film · Monolayer · Cubic phase · Inverted hexagonal phase · Surface tension

A. Jordanova · B. Tenchov (✉)
Institute of Biophysics, Bulgarian Academy of Sciences, Sofia 1113, Bulgaria
E-mail: tenchov@obzor.bio21.bas.bg

Z. Lalchev
Biological Faculty, Sofia University "St. Kliment Ohridski", 8 Dragan Tsankov Street, Sofia 1164, Bulgaria

Introduction

As a result of their amphiphilic structure, membrane lipids are able to spread at interfaces and to form various kinds of monolayers and foam films. The lipid behaviour at the air/water interface is of certain physiological relevance, at least for the reason that it determines the functioning of the lung surfactant. Studies carried out with vesicle dispersions have shown that spreading at interfaces, as well as the formation of lipid foam films, strongly depend on the vesicle phase state (Cohen et al. 1991; Exerowa and Nikolova 1992; Lalchev et al. 1994; Nikolova et al. 1994, 1996; Panaiotov et al. 1995; Vassilieff et al. 1996; Lalchev 1997). All parameters of importance, such as film thickness and homogeneity, threshold bulk lipid concentration required for formation of a stable foam film, film lifetimes, lateral lipid diffusion in foam films, rate of monolayer spreading, equilibrium surface tension, etc., were found to strongly differ between the lamellar gel (L_β) and the lamellar liquid crystalline (L_α) states of the vesicle dispersions. The observed effects have often been considered in terms of adhesion of whole vesicles to the interface, followed by their rupture and spreading, and have been interpreted as associated with surface phase transitions, which correspond to the melting transition in the bulk lipid phase. These findings clearly demonstrated that the phase state of the vesicle dispersion is an essential determinant of the lipid interfacial behaviour.

In addition to lamellar phases, some membrane lipids can also form non-lamellar liquid crystalline phases, typically represented by the inverse hexagonal phase H_{II} and several phases of cubic symmetry. Of particular interest among the cubic phases are the inverted bicontinuous phases Pn3m (Q^{224}), Im3m (Q^{229}) and Ia3d (Q^{230}), described as lipid bilayers draped along infinite periodic minimal surfaces (for reviews see, e.g., Andersson et al. 1988; Seddon and Templer 1995; Charvolin and Sadoc 1996; Luzzati 1997). The lipid bilayer forming a bicontinuous cubic phase divides the aqueous phase into two percolating and interpenetrating, but not connected to each other, spaces. The structure of the Pn3m phase is illustrated in Fig. 1. The significance of the L_α phase is well recognized: it represents the state of the lipid bilayer in the biological membranes, and various suggestions for possible physiological roles of the non-lamellar lipid patterns are under investigation (de Kruijff 1997; Luzzati 1997; Siegel 1999).

While the interfacial behaviour of vesicle dispersions has been the subject of numerous studies, no data appear to exist concerning formation of monolayers and foam films from non-lamellar lipid phases. The present work is the first attempt to address this issue. Our aim was to determine the kinetics of lipid spreading at the air/water interface and the probability for formation of stable foam films from inverted hexagonal and cubic phases, and to compare their surface behaviour with that of the lamellar phase. The measurements were carried out with the phospholipid dipalmitoleoylphosphatidylethanolamine (DPoPE). We used DPoPE as we found that this lipid is able to form not only L_α and H_{II} phases, but also a cubic Pn3m phase induced by temperature cycling at convenient temperatures and electrolyte conditions for monolayer and foam film studies.

Materials and methods

Preparation of lipid dispersions

1,2-Dipalmitoleoyl-*sn*-glycero-3-phosphoethanolamine (DPoPE) was purchased from Avanti Polar Lipids (Alabaster, USA) and used as received. Thin layer chromatography checks displayed a single lipid spot. Lipid dispersions in doubly distilled water and in 0.5 M NaCl (Merck) solutions were prepared at room temperature by mechanical agitation. Fully hydrated DPoPE forms a lamellar liquid crystalline phase L_α over a broad temperature range, from a melting transition taking place at about –35 °C up to 42 °C, where the dispersion transforms into the H_{II} phase (Fig. 2). As is typical for all lipids (Koynova et al. 1997), the latter transformation is slightly depressed by NaCl and takes place at 39 °C for DPoPE dispersions in 0.5 M NaCl solution. It is of importance for the present work that the $L_\alpha \rightarrow H_{II}$ transition is reversible, with a relatively large hysteresis of 10–15 °C (Fig. 2). After heating to the H_{II} range, followed by cooling to temperatures within the hysteretic loop, a DPoPE dispersion would reside in the supercooled H_{II} phase.

A cubic phase was prepared by temperature cycling of the lipid dispersion between 0 °C and 60 °C (Tenchov et al. 1998). Forty temperature cycles were sufficient to complete the conversion. As made clear by X-ray diffraction, the cubic phase prepared by this procedure is the inverse bicontinuous Pn3m (Q^{224}) phase (Fig. 3). The Pn3m phase replaces the initial L_α phase over its whole existence range. It also replaces the H_{II} phase up to 50–55 °C, where the cubic phase undergoes a reversible $Pn3m \leftrightarrow H_{II} + Pn3m$ phase transition (data not shown). The Pn3m phase of DPoPE induced by temperature cycling is stable for several weeks upon storage at room temperature; however, all measurements in the present work were made with freshly prepared Pn3m phases, within 2–3 h after their preparation.

Differential scanning calorimetry

Calorimetric control of the lipid dispersions was performed using a high-sensitivity differential adiabatic scanning microcalorimeter (DASM-4, Biopribor, Pushchino, Russia) with sensitivity better than 4×10^{-6} cal K^{-1} and a noise level less than 5×10^{-7} W. Heating and cooling runs were made at a scan rate of 0.5 °C min^{-1}. The thermograms shown in Fig. 2 were corrected for the instrumental baseline. The calorimetric enthalpy of the transitions was determined as the area under the excess heat capacity curve. The lipid concentration was 10–15 mg mL^{-1}.

X-ray diffraction

Identification of the DPoPE liquid crystalline phases was carried out at stations X-13 and A-2 at DESY, Hamburg, as described

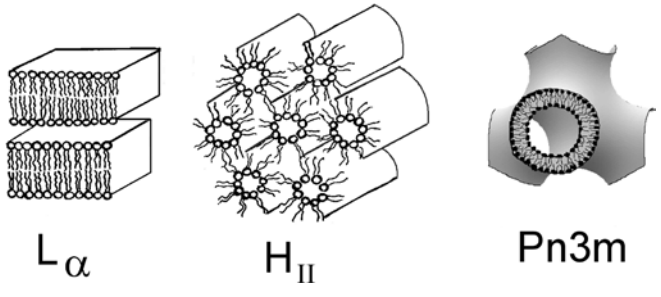

Fig. 1 Structures of the lipid liquid crystalline lamellar L_α, inverted hexagonal H_{II} and inverted bicontinuous cubic Pn3m phases

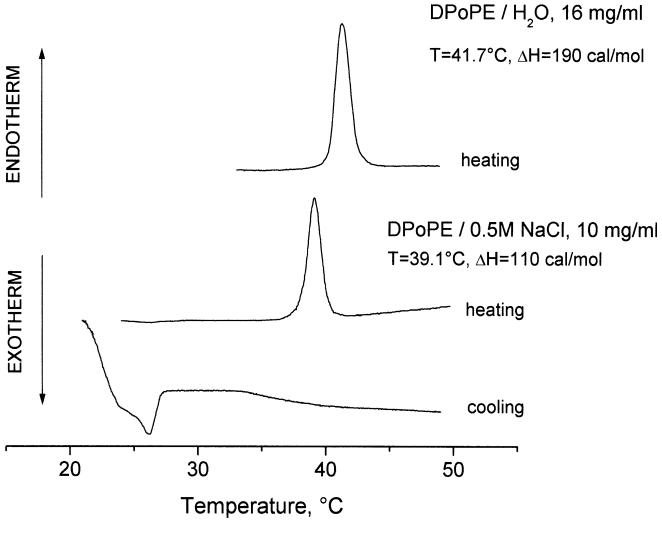

Fig. 2 DSC thermograms of the $L_\alpha \leftrightarrow H_{II}$ transition of DPoPE dispersions in water and 0.5 M NaCl solution. Scan rate 0.5°C min^{-1}

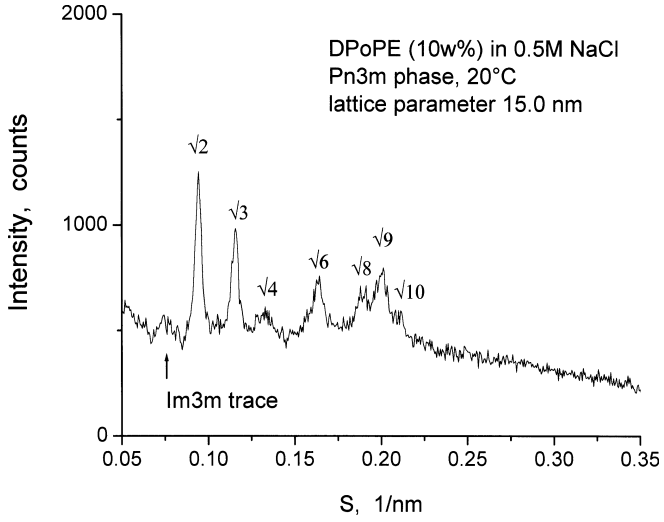

Fig. 3 Low-angle X-ray diffraction pattern of the DPoPE cubic Pn3m phase induced by temperature cycling, as described in Materials and methods. Lattice parameter 15.0 nm; 20 °C. The diffraction peak indexing is given in the figure. A hump (see *arrow*) in the pattern indicates the possible presence of a trace of the cubic Im3m phase in the dispersion

previously (Tenchov et al. 1998). The DPoPE concentrations used were 5–10 wt%.

DPoPE monolayers at the air/water interface

Monolayers were formed by spreading DPoPE dispersions in a Teflon trough with an area of 69 cm^2 (Biegler-Electronic, Austria) and the surface tension γ (mN m^{-1}) was followed with time by the Wilhelmy plate method. The DPoPE dispersions were applied with a syringe to final surface concentrations of 80, 40 and 20 $Å^2$ per lipid molecule over subphases of 0.5 M NaCl solution or doubly distilled water. A platinum float of size 1×1.6 cm was used. The trough temperature was controlled with a precision of ±0.5 °C. Experiments were carried out at 22 °C and 37 °C. The surface tension γ was measured with an accuracy of 0.5% and each measurement was repeated at least three times with different sample preparations.

DPoPE foam films

Black foam films (Fig. 4) were investigated by the microinterferometric method (Sheludko 1967) in its currently used version (Exerowa et al. 1992). Microscopic horizontal foam films of radius 0.2 mm were formed in a specially constructed glass cell in the middle of a biconcave drop. Equilibration for about 30 min before film formation was necessary to allow for phospholipid adsorption, vapour pressure saturation and temperature adjustment. The measuring cell was thermostatted with an accuracy within ±0.1 °C. It was equipped with an optical system for observation and investigation of foam films. At least 20 measurements were made at each temperature, with different sample preparations.

The bilayer foam films consist of two monolayers of amphiphilic molecules in a gaseous phase, which are in contact with each other through their polar head groups (Fig. 4C). After sucking the solution from the biconcave drop, the foam film initially forms as a thick film (thickness more than 100 nm) and further spontaneously becomes thinner. During film drainage, black spots may appear on its surface, resulting from local thinning; then these spots fuse and expand to fill up the entire film area. Two kinds of black foam films are known: common black films and Newton (bilayer) black films. The common black films contain a free water layer between the two monolayers and their thickness varies from ~10 to ~20 nm (Fig. 4B). The Newton black films, also called bilayer foam films, contain no free water (Fig. 4C). Their thickness is less than 8 nm. The formation of bilayer foam films depends on the electrolyte conditions. We used 0.5 M NaCl solutions for our measurements, where all the stable DPoPE films we observed were bilayer foam films.

Results and discussion

Spreading of lamellar and non-lamellar lipid phases at the air/water interface

The spreading behaviour of the lipid lamellar and non-lamellar phases was studied by adding appropriate amounts of the respective dispersion to the air/water interface and recording the decrease of surface tension γ with time. For valid comparisons to be made between the L_α, H_{II} and Pn3m phases of DPoPE, their spreading obviously needs to be recorded at the same temperature. This condition is readily met for the L_α and Pn3m phases. Since the latter phase replaces the former one over its whole temperature range of existence, their spreading kinetics can be compared at any temperature above 0 °C up to the $L_\alpha \rightarrow H_{II}$ transition temperature. We made measurements for these phases at 22 °C and 37 °C. With the H_{II} phase, this goal was achieved by making measurements at 37 °C, a temperature which is within the hysteretic loop of the $L_\alpha \leftrightarrow H_{II}$ transition. A freshly prepared L_α phase was heated to 60 °C to ensure its full conversion into the H_{II} phase. The H_{II} phase was then cooled to 37 °C and its spreading was recorded at that temperature. It should be noted that the supercooled H_{II} phase of DPoPE is stable at 37 °C for times much longer than the experiment duration. In principle, the spreading behaviour of the Pn3m and H_{II} phases can be also compared at temperatures above the $L_\alpha \rightarrow H_{II}$ transition, since the cubic phase continues to exist up to

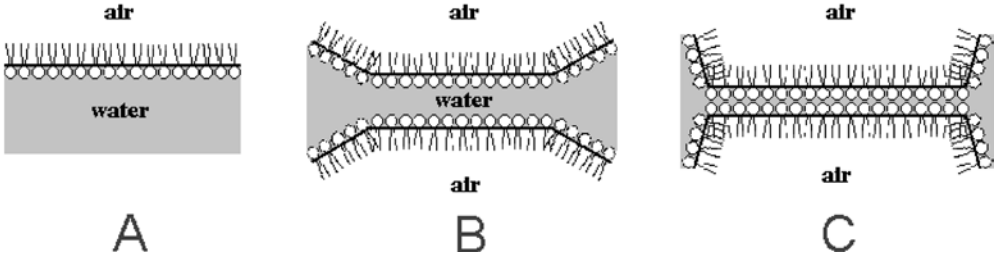

Fig. 4 Lipid monolayer (**A**); common black foam film (**B**); Newton (bilayer) black foam film (**C**)

50–55 °C. We did not make such comparisons, however, owing to the limited temperature control range of the monolayer trough.

The γ versus t curves recorded for three different surface concentrations (80, 40 and 20 Å^2 per lipid molecule) at 22 °C and 37 °C show that the surface tension decreases to a constant value in 1–3 min (Figs. 5 and 6). The best spreading, resulting in the lowest surface tension values, was observed for the L_α phase, followed by the Pn3m phase, and then by the H_{II} phase. The spreading of the latter phase was rather poor at all surface concentrations. The final surface tension strongly depends on the DPoPE surface concentration. In the range studied, it decreases from 50.9 to 26.5 mN m^{-1} for the L_α phase, and from 56.0 to 43.1 mN m^{-1} for the Pn3m phase at 22 °C. As could be expected, the final γ values for subphases with distilled water are higher than those for subphases with 0.5 M NaCl solutions, but the L_α phase again spreads better than the Pn3m phase (Fig. 5B). The spreading rate, $d\gamma/dt$, is highest for the L_α phase at all surface concentrations and temperatures, followed by the Pn3m and H_{II} phases. It thus appears that, with regard to their ability to spread at interfaces and to lower the surface tension, the lipid phases order as $L_\alpha > Pn3m > H_{II}$. The rather large differences found in the surface tension values clearly indicate that the non-lamellar phases and especially the H_{II} phase are substantially less prone to surface spreading and disintegration upon contact with an air/water interface.

Formation of bilayer foam films from lamellar and non-lamellar lipid phases

The propensity of the DPoPE lamellar and non-lamellar phases to form foam films was characterized by measuring the probability W for formation of stable films from these phases as a function of temperature and the bulk lipid concentration. By definition, $W = \Delta N/N$, where ΔN is the number of trials resulting in stable,

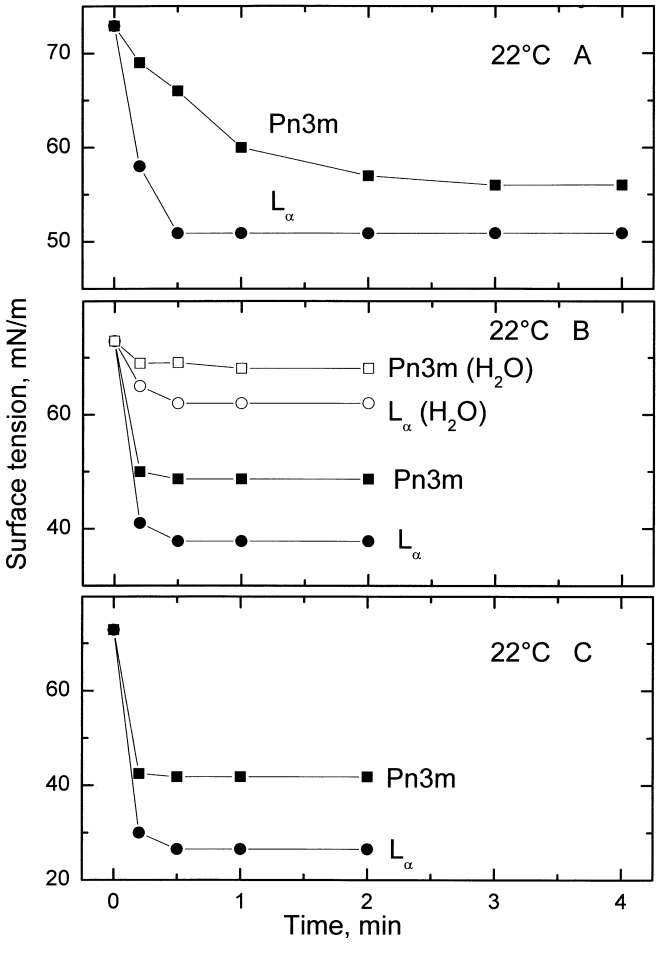

Fig. 5A–C Surface tension decrease caused by spreading of the L_α (*filled circles*) and Pn3m (*filled squares*) DPoPE phases on subphases of 0.5 M NaCl solution at 22 °C. The lipid surface concentrations in panels **A**, **B** and **C** are 80, 40 and 20 Å^2 per molecule, respectively. The *open symbols* in panel **B** indicate the values obtained upon lipid spreading on subphases of distilled water

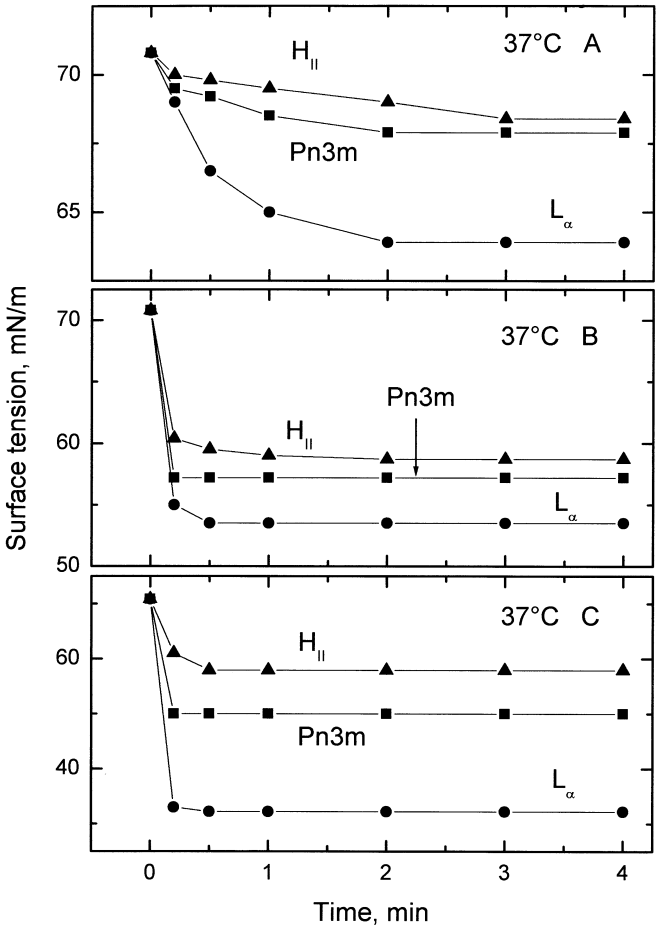

Fig. 6A–C Surface tension decrease caused by spreading of L_α (*filled circles*), Pn3m (*filled squares*) and H_{II} (*filled triangles*) DPoPE phases on subphases of 0.5 M NaCl solution at 37 °C. The lipid surface concentrations in panels **A**, **B** and **C** are 80, 40 and 20 Å^2 per molecule, respectively

long-lived (> 30 min) films, and N is the total number of trials. Accordingly, W assumes values from 0 to 1, these values reflecting film rupture or formation of a stable film, respectively. This quantity characterizes the film stability at any given electrolyte content, temperature and bulk lipid concentration. Following its definition, we measured the dependence of W on the bulk DPoPE concentration, C, for the Pn3m, L_α and H_{II} phases in 0.5 M NaCl at appropriate temperatures in the range 20–55 °C. At least 20 DPoPE films were formed from different sample preparations at each temperature and the accuracy of the C_t determination thus achieved was 4–6%. As is typical for phospholipids (Exerowa and Nikolova 1992; Nikolova et al. 1994, 1996), the W versus C curves obtained are step-like, precipitously changing from 0 to 1 in a very narrow concentration interval (Fig. 7). We can thus determine clear-cut threshold concentrations C_t for the three DPoPE phases studied at which W becomes equal to 1, i.e. where a stable foam bilayer forms in all trials. As can be seen from Fig. 7, the respective C_t values for the DPoPE phases are 20 μg mL^{-1} for L_α at 22 °C, 30 μg mL^{-1} for Pn3m at 22 °C and 45 °C, and 60 μg mL^{-1} for H_{II} at 45 °C.

A most important characteristic of the foam films is the temperature dependence of their threshold concentration C_t. A widely recognized theoretical description of bilayer film stability, based on the thermodynamic equilibrium between surfactant molecules in the film and surfactant monomers in the bulk phase, considers film rupture as the nucleation and growth of vacancies (holes) in the film (Kashchiev and Exerowa 1980, 1983). It predicts linear Arrhenius, $\ln C_t$ versus $1/T$, plots with slopes providing a measure of the amphiphile binding energy in the film, $Q/2kT = -\ln(C_t/C_0)$, where C_0 is a reference concentration, k is the Boltzmann constant, and T is the temperature. Although this model may not be directly applicable to our results, since the bulk phases studied here comprise both lipid aggregates and monomers, we nevertheless find it instructive to use Arrhenius plot representations for the temperature data. The C_t values for the L_α and H_{II} phases of DPoPE substantially increase with the temperature. Their Arrhenius plots are linear and intersect at 36–37 °C (Fig. 8). This temperature is by ~3 °C lower than the peak temperature of the $L_\alpha \rightarrow H_{II}$ transition and coincides with the onset temperature of the latter transition, as determined by DSC (Fig. 2). Noteworthy, the $L_\alpha \leftrightarrow H_{II}$ transition hysteresis is clearly reflected in the film behaviour. Measurements with supercooled H_{II} phases at temperatures within the hysteretic loop provide C_t values congruent with the Arrhenius plot for the H_{II} phase (filled triangles in Fig. 8). These data demonstrate that the foam film behaviour with temperature correlates well with the lipid bulk phase behaviour and precisely reflects the occurrence of a bulk lamellar-to-inverted hexagonal phase transformation, including its hysteresis in the cooling direction.

By contrast with films formed from L_α and H_{II} phases, however, we found that the threshold concentration of foam films prepared from the DPoPE cubic Pn3m phase does not change with the temperature. A constant, characteristic for this phase C_t value of 30 μg mL^{-1} was determined over the whole range studied between 20 °C and 50 °C (Fig. 8). This value does not depend on the direction of the stepwise temperature changes in the measuring cell. It was consistently recorded in both cooling and heating directions within the above temperature range. It may be noted in this connection that the lattice parameter of the cubic phases induced by temperature cycling is also temperature-insensitive over a broad temperature range, as demonstrated by X-ray diffraction (Tenchov et al. 1998). Although we believe this analogy is meaningful, it

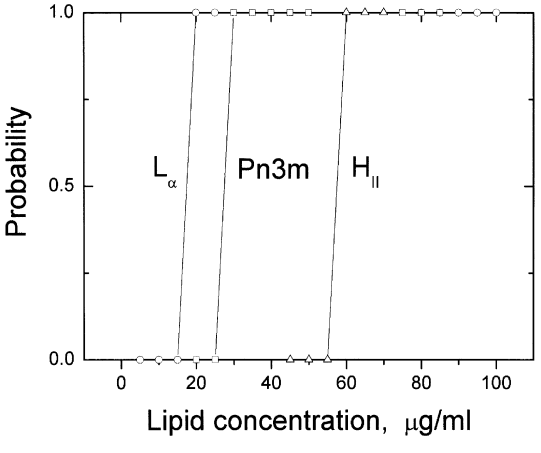

Fig. 7 Probability W for formation of bilayer foam films as a function of the lipid concentration for L_α (22 °C), Pn3m (22 °C and 45 °C) and H_{II} (45 °C) DPoPE phases in 0.5 M NaCl solution

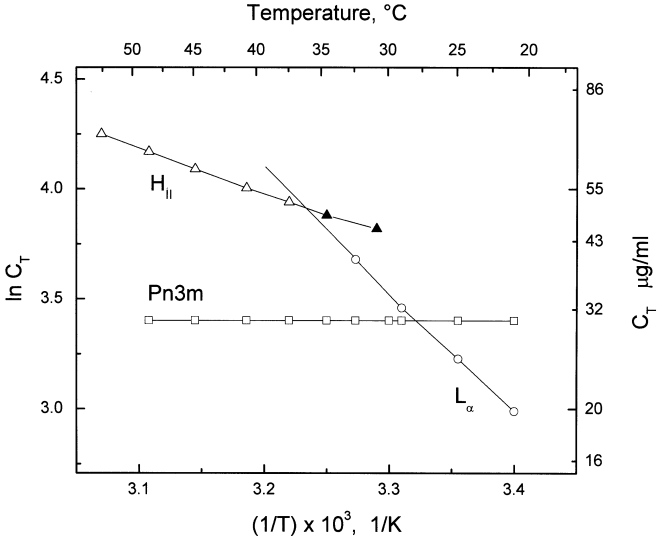

Fig. 8 Arrhenius plots of the threshold lipid concentrations C_t for formation of stable black foam bilayers from the Pn3m, L_α and H_{II} phases of DPoPE in 0.5 M NaCl solution

cannot be further pursued at this stage for the lack of unambiguous molecular models of the foam film formation from the bulk cubic phase. Figure 8 also shows that the horizontal C_t versus T plot for the Pn3m phase crosses the respective plot for the L_α phase at ~26 °C, i.e. at the temperature bounding from below the hysteresis range of the $L_\alpha \leftrightarrow H_{II}$ transition. As was shown in our previous study on induction of bicontinuous cubic phases by means of temperature cycling, a cubic phase, once formed, replaces the initial L_α phase over its whole temperature range of existence and does not spontaneously revert back to the L_α state. This behaviour leaves unanswered an important question: which of these two phases represents the thermodynamically stable state of the lipid dispersion? The present data on the stability of foam bilayers, formed from these two phases, provide grounds to consider the induced cubic phase Pn3m of DPoPE as more stable than the L_α phase at temperatures which are within the hysteretic loop of the $L_\alpha \leftrightarrow H_{II}$ transition, and the L_α phase as the more stable phase at temperatures below that loop. This supposition is consistent with the C_t versus T curves for the two phases given in Fig. 8 and also with our previous real-time X-ray measurements, which have shown that an increasing amount of the cubic phase only accumulates during the cooling step of the consecutive temperature cycles through the $L_\alpha \leftrightarrow H_{II}$ transition.

Conclusions

The present study, which appears to be the first one on the formation of monolayers and bilayer foam films from non-lamellar lipid phases, shows that the lamellar L_α, the inverted hexagonal H_{II} and the bicontinuous cubic Pn3m phase (induced by temperature cycling) of the phospholipid DPoPE display largely distinct interfacial behaviour. With regard to monolayer formation, the best spreading at the air/water interface, resulting in lowest values of the surface tension, was recorded for the L_α phase, followed by the Pn3m phase; the poorest spreading was observed for the H_{II} phase. According to their ability to lower surface tension and disintegrate at the air/water interface, the three phases order as $L_\alpha > Pn3m > H_{II}$. From measurements on the probability for formation of foam films from these phases, for each phase we have derived specific, clearly expressed threshold (minimum) bulk lipid concentrations C_t, required for the formation of stable foam bilayers. Their temperature dependence correlates well with the bulk lipid phase behaviour. The Arrhenius, $\ln C_t$ versus $1/T$, plots for the L_α and H_{II} phases are linear and intersect at ~36–37 °C, coinciding with the onset of the bulk $L_\alpha \rightarrow H_{II}$ phase transition, as determined by DSC. The plot for the H_{II} phase also contains a "metastable" portion, corresponding to the relatively large hysteresis in the latter transition. The C_t value for the Pn3m phase, equal to 30 μg mL^{-1}, was found to be constant over the whole range investigated between 20 °C and 50 °C. Since the horizontal C_t versus T plot for the Pn3m phase crosses the respective plot for the L_α phase at the temperature bounding from below the hysteretic loop of the $L_\alpha \leftrightarrow H_{II}$ transition (~26 °C), we surmise on this basis that a cubic phase induced by temperature cycling should be considered as thermodynamically stable relative to the initial L_α phase at temperatures within the hysteretic loop of the $L_\alpha \leftrightarrow H_{II}$ phase transition, and that the L_α phase should be considered as the stable phase at temperatures below that loop.

Acknowledgements The authors are grateful to Dr. Rumiana Koynova and Dr. Gert Rapp for help with the DSC and X-ray measurements. This work was partially supported by grant K-801/1998 from the Bulgarian National Science Fund.

References

Andersson S, Hyde S, Larsson K, Lidin K (1988) Minimal surfaces and structures: from inorganic and metal crystals to cell membranes and biopolymers. Chem Rev 88:221–242

Charvolin J, Sadoc J-F (1996) Ordered bicontinuous films of amphiphiles and biological membranes. Phil Trans R Soc Lond A 354:2173–2192

Cohen R, Koynova R, Tenchov B, Exerowa D (1991) Direct measurement of interaction forces in free liquid films stabilized with phosphatidylcholine. Eur Biophys J 20:203–208

De Kruijff B (1997) Lipids beyond the bilayer. Nature 386: 129–130

Exerowa D, Nikolova A (1992) Phase transitions in phospholipid foam bilayers. Langmuir 8:3102–3108

Exerowa D, Kashchiev D, Platikanov D (1992) Stability and permeability of amphiphile bilayers. Adv Colloid Interface Sci 40:201–456

Kashchiev D, Exerowa D (1980) Nucleation mechanism of rupture of Newtonian black films. J Colloid Interface Sci 77:501–511

Kashchiev D, Exerowa D (1983) Bilayer lipid membrane permeation and rupture due to hole formation. Biochim Biophys Acta 732:133–145

Koynova R, Brankov J, Tenchov B (1997) Modulation of the lipid phase behaviour by kosmotropic and chaotropic solutes. Experiment and thermodynamic theory. Eur Biophys J 25: 261–274

Lalchev Z (1997) Surface properties of lipids and proteins at biointerfaces. In: Birdi KS (ed) Handbook of surface and colloid chemistry. CRC Press, Boca Raton, Fla., USA, pp 625–687

Lalchev Z, Wilde P, Clark D (1994) Surface diffusion on phospholipid foam films. 1. Dependence of the diffusion coefficient in the lipid phase state, molecular length and charge. J Colloid Interface Sci 167:80–86

Luzzati V (1997) Biological significance of lipid polymorphism: the cubic phases. Commentary. Curr Opinion Struct Biol 7:661–668

Nikolova A, Exerowa D, Lalchev Z, Tsonev L (1994) Thermal transitions in dimyristoylphosphatidylcholine foam bilayers. Eur Biophys J 23:145–152

Nikolova A, Koynova R, Tenchov B, Exerowa D (1996) Chain-melting phase transition in dipalmitoylphosphatidylcholine foam bilayers. Chem Phys Lipids 83:111–121

Panaiotov I, Ivanova T, Balashev K, Proust J (1995) Spreading kinetics of dimyristoylphosphatidylcholine liposomes at the air/water interface below and above the main phase transition temperature. Colloids Surf A 102:159–165

Seddon J, Templer R (1995) Polymorphism of lipid-water systems. In: Lipowsky R, Sackmann E (eds) Handbook of biological physics. Elsevier, Amsterdam, pp 97–160

Sheludko A (1967) Thin liquid films. Adv Colloid Interface Sci 1:391–464

Siegel D (1999) The modified stalk mechanism of lamellar/inverted phase transitions and its implications for membrane fusion. Biophys J 76:291–313

Tenchov B, Koynova R, Rapp G (1998) Accelerated formation of cubic phases in phosphatidylethanolamine dispersions. Biophys J 75:853–866

Vassilieff C, Panaiotov I, Manev E, Proust J, Ivanova T (1996) Kinetics of liposome disintegration from foam film studies. Effect of the lipid bilayer phase state. Biophys Chem 58:97–107